EC
Journals.ASM.org

# Bradyzoite Pseudokinase 1 Is Crucial for Efficient Oral Infectivity of the *Toxoplasma gondii* Tissue Cyst

**Kerry R. Buchholz,[a] Paul W. Bowyer,[b]* John C. Boothroyd[a]**

Department of Microbiology and Immunology, Stanford University School of Medicine, Stanford, California, USA[a]; Department of Pathology, Stanford University School of Medicine, Stanford, California, USA[b]

**The tissue cyst formed by the bradyzoite stage of *Toxoplasma gondii* is essential for persistent infection of the host and oral transmission. Bradyzoite pseudokinase 1 (BPK1) is a component of the cyst wall, but nothing has previously been known about its function. Here, we show that immunoprecipitation of BPK1 from *in vitro* bradyzoite cultures, 4 days postinfection, identifies at least four associating proteins: MAG1, MCP4, GRA8, and GRA9. To determine the role of BPK1, a strain of *Toxoplasma* was generated with the *bpk1* locus deleted. This BPK1 knockout strain (Δ*bpk1*) was investigated *in vitro* and *in vivo*. No defect was found in terms of *in vitro* cyst formation and no difference in pathogenesis or cyst burden 4 weeks postinfection (wpi) was detected after intraperitoneal (i.p.) infection with Δ*bpk1* tachyzoites, although the Δ*bpk1* cysts were significantly smaller than parental or BPK1-complemented strains at 8 wpi. Pepsin-acid treatment of 4 wpi *in vivo* cysts revealed that Δ*bpk1* parasites are significantly more sensitive to this treatment than the parental and complemented strains. Consistent with this, 4 wpi Δ*bpk1* cysts showed reduced ability to cause oral infection compared to the parental and complemented strains. Together, these data reveal that BPK1 plays a crucial role in the *in vivo* development and infectivity of *Toxoplasma* cysts.**

The obligate intracellular parasite *Toxoplasma gondii* has two asexual developmental forms: the fast-growing tachyzoite and the slower-growing, cyst-forming bradyzoite. Both are necessary for propagation throughout its life cycle. Bradyzoites are a major source of human infection through ingestion of tissue cysts in undercooked meat or other tissue (1). Although the initial infection is generally controlled, the parasites are not cleared from the body and are able to persist for the lifetime of the host in bradyzoite-containing tissue cysts (1). This developmental form of *Toxoplasma* is of particular interest in respect to human infection and disease, as reactivation of latent cysts in the brain causes severe disease in immunocompromised individuals (1–3). Chemotherapies currently available act only upon the tachyzoite stage and are unable to clear the tissue cysts. Hence, a better understanding is needed of how bradyzoite cysts are established and maintained in the host.

The tissue cysts formed by bradyzoites are essential for transmission within the *Toxoplasma* life cycle via carnivorism. Cysts can range in size from less than 10 to 70 μm in diameter and contain from several to hundreds or even thousands of bradyzoites (4). The size of cysts is at least partially dependent on time postinfection, with larger cysts observed at later times (4). The cyst wall is relatively thin (<0.5 μm thick) and can be seen by electron microscopy as granular material that accumulates within the parasitophorous vacuole (PV) just below the parasitophorous vacuole membrane (PVM) (4). The cyst wall contains glycosylated material as indicated by the binding of *Dolichos biflorus* agglutinin lectin (DBA) which recognizes *N*-acetylgalactosamine (GalNAc) and succinylated-wheat germ agglutinin (S-WGA) which binds *N*-acetylglucosamine (GlcNAc) (5). It is thought that the cyst wall acts to protect the parasites from harsh environmental conditions during passage through the gastrointestinal (GI) system and perhaps aids in immune evasion. Despite the importance of the tissue cyst in the life cycle of *Toxoplasma gondii*, few components of the cyst wall have been identified, and nothing is known about their function (6–8).

Recently, we identified bradyzoite pseudokinase 1 (BPK1) (TGME49_253330 [ToxoDB v8.0]) as a component of the cyst wall expressed early in cyst formation (9). BPK1 contains a predicted kinase fold but lacks the residues essential for catalytic activity (9, 10). Far from being unimportant, inactive "pseudokinases" are known to regulate active kinases and signaling pathways and are thought to function as scaffolds facilitating multiprotein complexes (11).

To investigate what proteins BPK1 may interact with at the cyst wall, we performed immunoprecipitations using a strain of *Toxoplasma* engineered to express an epitope-tagged version of BPK1. To determine the function of BPK1 in the bradyzoite tissue cyst, we created a parasite line with the coding region of BPK1 deleted and investigated pathogenesis and cyst formation *in vitro* and *in vivo*. The results show that BPK1 is essential for proper cyst function *in vivo* and suggest that this bradyzoite-specific protein could have a scaffolding role in the cyst wall.

## MATERIALS AND METHODS

**Cell and parasite culture.** *Toxoplasma gondii* strains used in the study are described in Table 1. Parasites cultured under tachyzoite conditions were grown in confluent primary human foreskin fibroblasts (HFFs) in Dulbecco modified Eagle medium (DMEM) (Invitrogen, Carlsbad, CA) with 10% fetal bovine serum (FBS; HyClone, Logan, UT), 2 mM glutamine, 100 U/ml penicillin, and 100 μg/ml streptomycin (complete DMEM

Received 11 December 2012 Accepted 2 January 2013
Published ahead of print 4 January 2013
Address correspondence to John C. Boothroyd, john.boothroyd@stanford.edu.
* Present address: Paul W. Bowyer, Department of Pathogen Molecular Biology, London School of Hygiene and Tropical Medicine, London, United Kingdom.
Supplemental material for this article may be found at http://dx.doi.org/10.1128/EC.00343-12.

doi:10.1128/EC.00343-12

**TABLE 1** *Toxoplasma gondii* strains used in this study

| Strain | Strain genotype | Parental strain |
|---|---|---|
| PRU | PRUΔ*hxgprt* | N/A[a] |
| BPK1-tag | PRUΔ*hxgprt BPK1-venus-6xhis-3xflag*::*hxgprt* | PRUΔ*hxgprt* |
| Parental | PRUΔ*hxgprt*::*HXGPRT GRA2*P-*gfp TUB1*P-*luc* | PRUΔ*hxgprt GRA2*P-*gfp TUB1*P-*luc* (A7) |
| Δ*bpk1* | PRUΔ*hxgprt* Δ*bpk1*::*HXGPRT GRA2*P-*gfp TUB1*P-*luc* | PRUΔ*hxgprt GRA2*P-*gfp TUB1*P-*luc* (A7) |
| Complemented | PRUΔ*hxgprt* Δ*bpk1*::*HXGPRT BPK1*P-*BPK1*[b] *GRA2*P-*gfp TUB1*P-*luc* | PRUΔ*hxgprt* Δ*bpk1 GRA2*P-*gfp TUB1*P-*luc* |

[a] N/A, not applicable.
[b] BPK1 coding and 2,000 bp upstream (promoter).

[cDMEM]) at 37°C with 5% $CO_2$. Differentiation to the bradyzoite form was induced by growth under low-serum, alkaline conditions in ambient (low) $CO_2$ essentially as described previously (12). Briefly, confluent monolayers of HFFs were infected with tachyzoites at a multiplicity of infection (MOI) of 1 for 4 h in cDMEM at 37°C with 5% $CO_2$. The cells were washed twice with phosphate-buffered saline (PBS) and cultured in bradyzoite medium (RPMI 1640 medium [Invitrogen] lacking sodium bicarbonate and lacking L-glutamine with 1% FBS, 10 mg/ml HEPES, 100 U/ml penicillin, and 100 μg/ml streptomycin [pH of the medium, 8.0]) and grown at 37°C without supplemented $CO_2$ to induce differentiation to the bradyzoite form (12).

**Generation of BPK1 knockout strain.** All primers used for these studies can be found in Table S1 in the supplemental material. A targeting plasmid was engineered to generate a *Toxoplasma* strain where the *BPK1* locus was replaced with the hypoxanthine-xanthine-guanine phosphoribosyltransferase selectable marker (*HXGPRT*) using the pTKO2 vector (13; C. E. Caffaro, A. A. Koshy, L. Liu, G. M. Zeiner, C. B. Hirschberg, and J. C. Boothroyd, submitted for publication). Briefly, ~1- to 2-kb regions immediately up- or downstream of the *BPK1* gene's start and stop codons were inserted flanking a cassette for expression of the selectable marker (*HXGPRT*). The plasmid was linearized by digestion with the NotI enzyme, and 10 to 30 μg was transfected by electroporation as previously described (14) into *Toxoplasma* PRUΔ*hxgprt GRA2*P-*gfp TUB1*P-*luc* strain A7 (15) which had been growing for 24 h under bradyzoite conditions. After transfection, the parasites were added to a 24-well plate with a confluent HFF monolayer and allowed to infect the cells for 4 h in cDMEM under tachyzoite growth conditions (as described above) prior to 2 washes with PBS and addition of bradyzoite medium as described above and growth under low $CO_2$ conditions. After 24 h, cDMEM containing mycophenolic acid (MPA) (50 μg/ml) and xanthine (XAN) (50 μg/ml) was added to select for stable integration as previously described (16), and the culture was allowed to grow under tachyzoite conditions. Populations were screened by PCR for homologous recombination of the vector, and single clones were isolated by limiting dilutions. To confirm the removal of the *BPK1* locus, genomic DNA was screened by PCR using primers within the vector and within the genomic sequence but outside the region used for targeting (Table S1) and confirmed by sequencing. To transfer (complement) the *BPK1* locus back into the knockout strain, the hypoxanthine-xanthine-guanine phosphoribosyltransferase (HXGPRT) locus was first removed using Cre recombinase as previously described (Caffaro et al., submitted). Briefly, a plasmid expressing Cre recombinase was transiently transfected into the Δ*bpk1* strain to catalyze recombination at the *loxP* sites flanking the *HXGPRT* marker in the pTKO2 vector. After growth in 350 μg/ml 6-thioxanthine to select for loss of *HXGPRT*, single clones were isolated by limiting dilutions. Excision of HXGPRT was confirmed by PCR. This clone was then used to generate the *BPK1*-complemented strain as follows. A plasmid containing the coding region of *BPK1* plus 2,000 bp 5′ of the start codon was made in the pTKO2 plasmid that had been modified so that it lacked mCherry. This plasmid was linearized and transfected as described above into the Δ*bpk1*parasites lacking the *HXGPRT* marker (due to Cre-mediated recombination) and integration of the new pTKO2 plasmid carrying BPK1 was selected for by using MPA-xanthine as described above.

**Generation of epitope-tagged BPK1.** All primers used can be found in Table S1 in the supplemental material. A targeting plasmid was engineered to generate a *Toxoplasma* strain in which the endogenous *BPK1* locus was replaced with one fused to a C-terminal venus-6×His-3×FLAG tag using the pTKO-VFTAP vector (17). Briefly, ~1- to 2-kb regions immediately up- or downstream of the *BPK1* gene's stop codon, but not including the stop codon, was inserted flanking the tag-coding sequence and the *HXGPRT* selectable marker. The targeting plasmid was linearized by digestion with the NotI enzyme, and 15 to 30 μg of plasmid was transfected by electroporation as previously described by Soldati and Boothroyd (14) into *Toxoplasma* PRUΔ*hxgprt* (D. Soldati, University of Geneva, Geneva, Switzerland) after incubation of extracellular parasites for 4 h at room temperature in cDMEM. Mycophenolic acid (50 μg/ml) and xanthine (50 μg/ml) were used to select for stable integration as previously described (16), and clones were isolated by limiting dilutions. To confirm a double recombination event, selected clones were screened for the absence of the negative selection marker mCherry. Correct integration was confirmed by PCR and sequencing.

**Immunoprecipitation assay. (i) Immunoprecipitation for protein identification.** Confluent monolayers of HFF cells in 15-cm dishes were infected with the *T. gondii* strain BPK1-tag (VFTAP) at a MOI of ~1 and grown under bradyzoite conditions as described above. At 4 days postinfection (dpi), the infected cells were washed once with cold PBS, once with cold TGK buffer (50 mM Tris [pH 8.0], 150 mM KCl, 10% glycerol) and once with cold TGK buffer plus protease inhibitors (cOmplete, EDTA-free; Roche, South San Francisco, CA). The cells were scraped off the plates, syringe lysed on ice by consecutive passage through 18-, 23-, 25-, and 27-gauge needles, and NP-40 (nonylphenyl polyethylene glycol) alternative detergent (EMD Millipore, Billerica, MA) was added to a final concentration of 0.1%. After 10-min incubation on ice, the insoluble fraction was removed by spinning 5 min at maximum speed in a microcentrifuge. Dynabeads (Sigma, St. Louis, MO) conjugated to M2 mouse anti-3×FLAG antibody (2.5 mg) were added to the soluble fraction, and the mixture was incubated for 40 min at 4°C. The beads were washed 4 times in TGK buffer with 0.1% NP-40 alternative and protease inhibitors. The proteins were eluted from the antibody with 200 μg of 3×FLAG peptide (Sigma), and the solution was added to 30 μl Talon Dynabead slurry (Invitrogen) equilibrated in TGK buffer with 0.1% NP-40 alternative detergent and protease inhibitors to remove bound proteins from the peptide. The beads were washed 4 times as described above, transferred to a new tube, and eluted 3 times, 10 μl each, in 1× SDS loading buffer (2× SDS sample buffer, 125 mM Tris-HCl [pH 7.0], 4% SDS, 20% glycerol, 0.005% bromophenol blue) with 150 mM imidazole at 70°C for 10 min. The entire product of the coimmunoprecipitation (co-IP) was run on a 4 to 12% NuPAGE Bis-Tris minigel (Invitrogen) in 1× NuPAGE MOPS SDS running buffer (Invitrogen) and stained with GelCode blue stain reagent (Thermo Scientific, Rockford, IL). The lane was cut into 14 slices and subjected to in-gel digestion with trypsin as described previously (18) before analysis on an LTQ ion trap mass spectrometer (ThermoFisher).

**(ii) LC-MS/MS.** Liquid chromatography coupled to tandem mass spectrometry (LC-MS/MS) was performed as described previously (19). Briefly, peptides were separated on a Basic Picofrit $C_{18}$ capillary column coupled to an Eksigent NanoLC-2D pump before analysis on an LTQ ion

trap mass spectrometer (Thermo Scientific). An acetonitrile gradient (0 to 60% in a 0.1% solution of formic acid over 2 h) was used to elute peptides at a flow rate of 250 nl/min, and the spray voltage was 2.0 kV. Dynamic exclusion was enabled for 180 s.

Data analysis was conducted as described previously (20). RAW files were generated for each gel slice by XCalibur (Thermo Scientific version 2.0). These files were analyzed using the Sequest algorithm in Bioworks (Thermo Scientific version 3.3) software package. Searches were performed against a custom concatenated target-decoy database containing the annotated proteins based on the *T. gondii* ME49 release 5 sequences (http://toxodb.org) and *Cryptosporidium parvum* database (http://cryptodb.org). SEQUEST data from each gel band were filtered and sorted using DTASelect version 1.9 (21) DTASelect and Contrast tools for assembling and comparing protein identifications (default settings).

**(iii) Immunoprecipitation for probing by immunoblotting.** Immunoprecipitations were performed as described above except after incubation with the M2 antibody-conjugated Dynabeads and 4 washes with TGK buffer with 0.1% NP-40 and protease inhibitors, proteins were eluted by 10-min incubation with 50 μl of 1× SDS-PAGE loading buffer containing dithiothreitol (DTT) at 70°C. The eluted samples were run on 4 to 12% NuPAGE Bis-Tris minigel in 1× MOPS running buffer prior to probing with antibodies as described above.

**(iv) Reciprocal coimmunoprecipitations.** Lysates from 4-day bradyzoite cultures of parasites endogenously C-terminally tagged with hemagglutinin (HA) using the pTKO vector (9) in 15-cm dishes were prepared as described above. Equal volumes of the soluble fraction of the lysate were incubated with 10 μl sera (rabbit polyclonal antibodies to GRA9 [22] or mouse polyclonal antibodies to MCP4 or MAG1 [see below], polyclonal rabbit anti-glial fibrillary acidic protein [anti-GFAP; Agilent Technologies, Santa Clara, CA], or normal sera of the same species) or 10 μg anti-GRA8 monoclonal antibodies (23) or mouse anti-ZO-1 (antibody against zonula occludens 1; Invitrogen) for 30 min while rotating at 4°C. Then 150 μg of protein G Dynabeads (Invitrogen) was added, and the mixture was incubated for 20 min while rotating at 4°C. The beads were washed 4× with TGK buffer containing 0.1% NP-40 and protease inhibitors. The beads were transferred to a new tube and eluted 2× with 15 μl each of 1× SDS-PAGE loading buffer containing DTT.

**Immunoblot assay.** Parasites were lysed from HFFs by multiple passages through a 27-gauge needle. Equal numbers of parasites were resuspended in SDS-PAGE loading buffer plus DTT, boiled 10 min, and frozen at −20°C prior to separation on a 10% SDS-PAGE gel or 4 to 12% NuPAGE Bis-Tris minigel (Invitrogen). All incubations were performed in Tris-buffered saline (TBS) with 5% milk and 0.05% Tween 20, unless otherwise noted, and were followed by the appropriate secondary antibody conjugated to horseradish peroxidase (HRP). Immunoblot analysis was performed by standard methods with the following antibodies: monoclonal antibody 3F10 (rat anti-HA antibody) conjugated to horseradish peroxidase (Roche, South San Francisco, CA), mouse monoclonal (M2) anti-3×FLAG (Sigma), rabbit anti-SAG2X (24) in 5% bovine serum albumin (BSA) in TBS, rabbit anti-SAG1, rabbit anti-GRA9 in 5% BSA in TBS (22), mouse monoclonal (A3.2) anti-GRA8 (23) in TBS, and rabbit anti-GRA7 in TBS (25). Mouse anti-BPK1, mouse anti-MAG1, and mouse anti-MCP4 were generated as described below.

**Generation of polyclonal antibodies.** N-terminal glutathione *S*-transferase (GST)-tagged proteins were expressed using the pGEX-6P1 plasmid (Agilent Technologies). GST-tagged BPK1, MAG1, and MCP4 (N-terminal repeat region, amino acids 31 to 536) were generated using the primers described in Table S1 in the supplemental material. All exclude the predicted signal peptide. The resulting fusion proteins were purified from *Escherichia coli* (Rosetta strain; Novagen/EMD Millipore) essentially as described previously (26) and injected intraperitoneally (i.p.) into BALB/c mice with 100 μl of RIBI conjugate (Corixa, Hamilton, MT) in a total volume of 200 μl. The initial dose was 100 μg protein/mouse, followed by 40 to 50 μg protein/mouse on days 21, 50, and 71 (BPK1, days 21, 35, and 63) after the initial injection. Serum was isolated on days 35, 61, and 85 (BPK1, days 35, 61, and 77) after the initial injection. All animal experiments were conducted with the approval and oversight of the Institutional Animal Care and Use Committee at Stanford University.

**Immunofluorescence assays.** *Toxoplasma*-infected HFF cells on glass coverslips were fixed with 3.5% formaldehyde for 20 min. All subsequent incubations were performed in PBS supplemented with 3% BSA. The cells were blocked in 3% BSA in PBS overnight at 4°C or at room temperature for 1 h and then permeabilized for 30 min with PBS supplemented with 0.3% to 0.5% Triton X-100. After incubation for 1 to 2 h with DBA-rhodamine (Vector Labs, Burlingame, CA) and the primary antibody, Alexa Fluor 594-conjugated secondary antibodies were used (Molecular Probes/Invitrogen). DBA was used as a marker of the cyst wall. Samples were viewed on an Olympus BX60 upright fluorescence microscope with a 100× oil immersion lens, and images were acquired with Image-Pro Plus software or QCapture software (version 2.9.11.2). Images were minimally and equally adjusted within groups using Adobe Photoshop CS3. To determine the two-dimensional area of the cyst, images were analyzed using ImageJ software.

**Mouse infection.** Female CBA/J mice ~8 to 10 weeks old were infected intraperitoneally with $2.5 \times 10^4$ tachyzoite parasites in 200 μl PBS. To generate cysts for oral infection, ~8- to 20-week-old female CBA/J mice were infected with $2.5 \times 10^4$ to $1 \times 10^5$ parasites as described above (mice were of the same age within each experiment). The brain was rinsed in PBS supplemented with 3% FBS (3% FBS/PBS), passed through a 100-μm cell strainer using the plunger of a 6-ml syringe, rinsed with 3% FBS/PBS, and stored on ice until it could be centrifuged at 500 × *g* for 15 min. The brain was washed with 3% FBS/PBS and fixed in 4% formaldehyde, and 1/10th of the material was stained with DBA conjugated to rhodamine in a volume of 500 μl. The samples were aliquoted into 96-well plates, and cysts were counted on an inverted Nikon Eclipse TE300 fluorescence microscope with a 20× objective. To determine cyst diameter, images of cysts were taken with QCapture software (version 2.9.11.2), and the diameters of the cysts (relative units) were measured using Adobe Photoshop CS3. Three diameter measurements were taken per cyst (length, width, and diagonal) and averaged to get a single value for each cyst. Ten to 20 or more cysts were analyzed per brain sample.

To orally infect mice with *in vivo Toxoplasma* cysts, a volume of brain material corresponding to 100 or 250 cysts, prepared, and counted as described above but without fixation, was placed on mouse chow in a plastic dish and given to individual 8- to 10-week-old female CBA/J mice (their food was removed from their cage the night before).

**Isolation of *in vivo* bradyzoite cysts.** The method used to purify bradyzoite cysts from mouse brains was modified from a previously described protocol (27). Briefly, the brain was passed through a 100-μm cell strainer as described above, washed once in 3% FBS/PBS, and brought up to 9 ml in 3% FBS/PBS. The suspension was passed through an 18-gauge needle prior to layering on top of a density gradient of (from bottom to top) 9 ml of 90% (vol/vol) Percoll in PBS (GE Healthcare, Piscataway, NJ) and 9 ml of 30% Percoll in a 50-ml conical tube and centrifuged at 1,200 × *g* for 15 min at 4°C. The cysts were harvested from the 30% layer and 30%/90% interface by removing and discarding the top brain suspension layer and then gentle aspiration to remove the bottom layer. The cyst suspensions were washed with PBS by bringing the volume up to 45 ml with 3% FBS/PBS and centrifuging at 1,500 × *g* for 15 min at 4°C. The supernatant was removed until ~5 ml remained, and this was then transferred to a 15-ml conical tube and washed again in 3% FBS/PBS. The supernatant was removed until ~0.5 ml remained, and this was used to resuspend the pellet which was then transferred to a 1.5-ml microcentrifuge tube and brought to 1.5 ml with 3% FBS/PBS and spun at 2,000 × *g* for 10 min. An aliquot of the isolated cysts was removed and stained with DBA-rhodamine, and cysts were counted on an inverted Nikon Eclipse TE300 fluorescence microscope using a 20× objective.

**Pepsin digestion and plaque assay.** Ten to 30 cysts isolated via Percoll gradients as described above were suspended in RPMI 1640 to a final

volume of 750 μl. An equal volume of warm (37°C) pepsin digestion solution (170 mM NaCl, 60 mM HCl, 0.1 mg/ml pepsin added fresh prior to use) was added and mixed by pipetting up and down. Aliquots of 500 μl were removed at 30 s and 10 min and neutralized with 130 μl of 94 mM $Na_2CO_3$ prior to plaquing 100 μl onto confluent HFFs in a 25-$cm^2$ flask in triplicate. Two hundred microliters was reserved for DNA extraction with DNeasy blood and tissue kit (Qiagen). Quantification of parasite genomes was performed by quantitative PCR (qPCR) amplification of the B1 gene (28) (forward, 5′-TCCCCTCTGCTGGCGAAAAGT-3′; reverse, 5′-AGC GTTCGTGGTCAACTATCGATTG-3′) in FastStart SYBR green master mix (Roche) according to the manufacturer's instructions, and comparison to a standard curve of tachyzoite DNA extracted from a known quantity of parasites.

## RESULTS

**Epitope-tagged BPK1 is secreted by parasites and localizes to the cyst wall.** The pseudokinase BPK1 is a component of the cyst wall that is secreted by bradyzoites and accumulates between the parasites and the PVM (9). The function of BPK1 in the cyst is unknown, but pseudokinases can have scaffolding or regulatory roles, so we first sought to identify the proteins with which BPK1 might be interacting. To do this, a *Toxoplasma* strain with a tandem venus, 6×His, and 3×FLAG epitope tag incorporated into the C terminus of the endogenous gene was created (strain BPK1-tag) and used for coimmunoprecipitation (co-IP) studies. To determine whether the BPK1 tag was expressed with the appropriate developmental control, BPK1-tag parasites were grown for 2 days under tachyzoite or bradyzoite conditions or 4 days under bradyzoite conditions, lysed from the host cells, counted, and analyzed by immunoblotting for the 3×FLAG tag of the BPK1. As a check on the efficient differentiation to bradyzoites, the immunoblot was also probed for surface antigens specific to the tachyzoite and bradyzoite stages (SAG1 and SAG2X, respectively), and the expected changes in abundance were observed (Fig. 1A). Immunoblotting with anti-3×FLAG antibodies demonstrated that the C-terminal epitope-tagged BPK1 is expressed and detected in BPK1-tag parasites (Fig. 1A, lanes 4 to 6), but not in the control strain (Fig. 1A, lanes 1 to 3). Importantly, the tagged BPK1 was upregulated in parasites grown under bradyzoite conditions compared to tachyzoite conditions (Fig. 1A, lanes 4 to 6). While some tagged BPK1 was expressed under tachyzoite cultures (Fig. 1A, lane 4), this is readily explained by the low level of bradyzoite differentiation (~10 to 20%) that occurs in tachyzoite cultures as previously described (9), and similarly low levels of BPK1 expression were observed in wild-type tachyzoite cultures using anti-BPK1 antiserum (data not shown).

To determine whether the endogenously tagged BPK1 is secreted by bradyzoites and localizes normally within the cyst, BPK1-tag and control (PRU) parasites were grown for 4 days under bradyzoite conditions prior to fixation and immunofluorescence assay (IFA) analysis. Tagged BPK1 was secreted from the parasites and localized to the periphery of the cyst coincident with the cyst wall as detected with DBA (Fig. 1B). No BPK1-venus signal was detected in the control, untagged cysts (data not shown). The localization of the tagged BPK1 is consistent with that seen using anti-BPK1 sera in the untagged strain (Fig. 1C) and previous data with HA-tagged BPK1 (9). Thus, tagged BPK1 is secreted from the parasites and localizes as expected to the cyst wall area.

**BPK1 coimmunoprecipitates with cyst- and membrane-associated proteins.** To determine what proteins BPK1 may complex with, we pursued a strategy of coimmunoprecipitation and LC-MS/MS. BPK1 was immunoprecipitated from the total protein lysate of 4 dpi *in vitro* bradyzoites grown on HFF monolayers using a modified tandem affinity purification method and the C-terminal 3×FLAG and 6×His tags (as described in Materials and Methods). The product of the co-IP was run on a 4 to 12% Bis-Tris gel, and the entire lane was cut into 14 pieces for protein identification by LC/MS-MS (Fig. 2A). In addition to BPK1 itself, six *Toxoplasma* proteins were identified that had at least 8 spectral counts and four different peptides were detected (Fig. 2B). These included two dense granule proteins which associate with the PVM or the intravacuolar network (IVN) of membranes, GRA8 and GRA9, and the cyst matrix and wall protein, MAG1 (8, 22, 23). These three proteins are relatively well studied and have had antibodies raised against them (8, 22, 23). GRA8 and MAG1 are present at the periphery of the vacuole or the cyst wall similar to BPK1 (8, 29). GRA9 is part of the IVN of tachyzoite vacuoles (22), but its localization is unknown in bradyzoite cysts. IFA analysis of 4 dpi *in vitro* cysts found that GRA8 and GRA9 colocalize with tagged BPK1, whereas the surface antigen SAG2X does not (Fig. 3). Thus, GRA8, GRA9, and MAG1 were prioritized for further study. The three other *Toxoplasma* proteins identified, *T. gondii* HSP70 (TgHSP70)/BiP (30), a multi-SRS-domain-containing protein (SRS44), and the microneme protein *T. gondii* SPATR (TgSPATR)

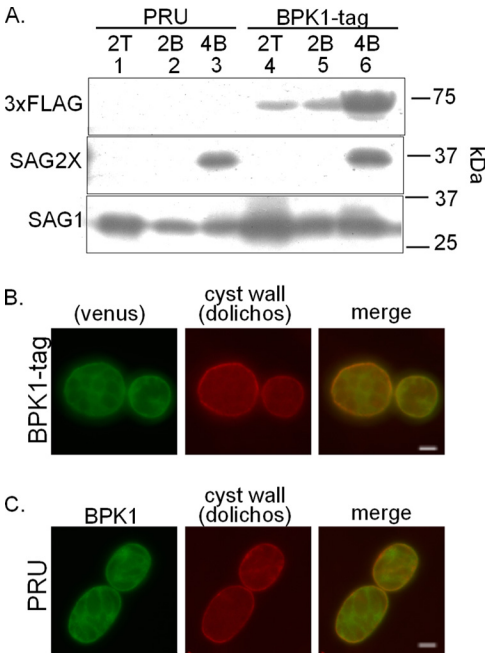


**FIG 1** Endogenously tagged BPK1 is upregulated and secreted by bradyzoites. (A) HFF monolayers were infected with PRUΔ*hxgprt* parasites or parasites expressing a BPK1 gene endogenously C-terminally tagged with a tandem venus-3×FLAG-6×His (BPK1 tag) for 2 days under tachyzoite growth conditions and 2 days and 4 days under bradyzoite growth conditions for analysis by SDS-PAGE. A total of $1 \times 10^6$ parasite equivalents were loaded per lane and probed with antibodies for 3×FLAG, SAG2X, or SAG1 as described in Materials and Methods. (B and C) Parasites were grown on HFF monolayers on glass coverslips for 4 days under bradyzoites growth conditions prior to fixation. (B) *Dolichos biflorus* agglutinin (DBA [red]) and the BPK1 tag (venus [green]) are indicated. (C) DBA (red) and anti-BPK1 (green) are indicated. Representative images from at least two independent experiments are shown in panels B and C. Bars, 5 μm.

A.

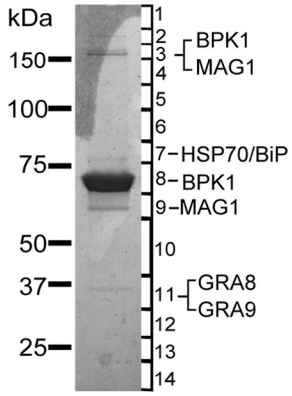


B. Spectral Counts

| | | | Band Number | | | | | | | | | | | | | | |
|---|---|---|---|---|---|---|---|---|---|---|---|---|---|---|---|---|---|
| | MM* | Gene ID | 1 | 2 | 3 | 4 | 5 | 6 | 7 | 8 | 9 | 10 | 11 | 12 | 13 | 14 | total |
| **BPK1** | 76.5** | TGME49_253330 | 16 | 15 | 25 | 8 | 19 | 14 | 45 | 103 | 70 | 23 | 8 | 3 | 2 | 3 | **354** |
| GRA7 | 25.9 | TGME49_203310 | - | - | - | - | - | - | - | - | - | - | - | 4 | - | - | 4 |
| no hom | 21.3 | TGME49_213880 | - | - | - | - | - | - | - | - | - | - | - | 3 | - | - | 3 |
| GRA3 | 23.9 | TGME49_227280 | - | - | - | - | - | - | - | - | - | - | - | 2 | - | - | 2 |
| no hom | 45.4 | TGME49_225160 | - | - | - | - | - | - | - | - | - | 3 | - | - | - | - | 3 |
| no hom | 47.7 | TGME49_279100 | - | - | - | - | - | - | - | - | - | 2 | - | - | - | - | 2 |
| no hom | 140 | TGME49_209755 | - | 3 | - | - | - | - | - | - | - | 2 | - | - | - | - | 5 |
| **HSP70/BiP** | 73.3 | TGME49_311720 | - | - | 5 | - | - | 6 | 28 | - | - | - | - | - | - | - | **39** |
| no hom | 102 | TGME49_258870 | - | - | - | - | - | 3 | - | - | - | - | - | - | - | - | 3 |
| **MAG1** | 49.1 | TGME49_270240 | 6 | 7 | 8 | 8 | 3 | - | 3 | - | 13 | - | - | - | - | - | **48** |
| **GRA9** | 35.3 | TGME49_251540 | - | - | - | - | 2 | - | - | - | - | - | 27 | - | - | - | **29** |
| **GRA8** | 28.6 | TGME49_254720 | - | - | - | - | - | - | - | - | - | - | 8 | - | - | - | **8** |
| actin | 41.9 | TGME49_209030 | - | - | - | - | - | - | - | - | - | - | 2 | - | - | - | 2 |
| **TgSPATR** | 97.1 | TGME49_204340 | - | - | - | - | 8 | - | - | - | - | - | - | - | - | - | **8** |
| no hom | 80.5 | TGME49_254470 | - | - | 2 | - | 2 | - | - | - | - | - | - | - | - | - | 4 |
| **SRS44** | 251 | TGME49_264660 | 9 | - | - | - | - | - | - | - | - | - | - | - | - | - | **9** |
| no hom | 328 | TGME49_215910 | 5 | - | - | - | - | - | - | - | - | - | - | - | - | - | 5 |
| no hom | 246 | TGME49_217680 | 2 | - | - | - | - | - | - | - | - | - | - | - | - | - | 2 |
| no hom | 54.8 | TGME49_208830 | - | 2 | - | - | - | - | - | - | - | - | - | - | - | - | 2 |
| ppg3 | 202 | TGME49_231960 | - | 3 | - | - | - | - | - | - | - | - | - | - | - | - | 3 |

* MM (molecular mass in kDa) estimate from ToxoDB v. 8.0 (includes signal peptide)
** estimated MM of BPK1 with tag

**FIG 2** Immunoprecipitation of BPK1 and LC-MS/MS identification of interacting proteins. HFF cells were infected with the *T. gondii* BPK1-tag strain for 4 days under bradyzoite conditions, and tandem affinity purification of BPK1 was performed using the 3×FLAG and 6×His tags as described in Materials and Methods. (A) GelCode blue-stained gel showing the eluate from the immunoprecipitation along with the approximate band limits for each slice analyzed by LC-MS/MS. The predominant constituents of the visible bands are indicated to the right. (B) Spectral counts of identified proteins in relation to gel slice (band number). A hyphen indicates that no spectral counts were identified. Boldface indicates at least eight spectral counts and four different peptides identified. Gene ID numbers from ToxoDB version 8.0 are shown. Data for all proteins with 2 or more spectral counts are shown. no hom, no homolog.

(31, 32), were not further pursued, so no conclusion as to the specificity of their interaction with BPK1 can be drawn here.

To confirm the specificity of the BPK1 interaction with the three selected proteins, co-IP was repeated using antibodies specific for the 3×FLAG epitope starting with 4 dpi *in vitro* bradyzoite cultures, and the eluate was analyzed by immunoblotting. GRA8, GRA9, and MAG1 were found to co-IP with BPK1 in the epitope-tagged strain but were not specifically detected in the untagged (PRU) control (Fig. 4A, lanes 3 and 4). The specificity of their interaction with BPK1 was further demonstrated by the fact that neither the abundant, PVM-associated dense granule protein GRA7 (33) nor the abundant bradyzoite surface antigen SAG2X (24) were specifically coprecipitated (Fig. 4A, lane 4). This indicates that the interaction of BPK1 with GRA8, GRA9, and MAG1 is not due to nonspecific precipitation of large portions of parasite debris or vacuolar membrane.

The microneme adhesive repeat (MAR) domain-containing protein 4 (MCP4), which contains a putative sialic acid-binding motif (34), is also a known component of the bradyzoite cyst wall (9). While it was not identified in the initial screen for BPK1-interacting partners, MCP4 runs at approximately 75 kDa (9). This is similar in size to the tagged BPK1 used here, and thus, any MCP4 signal could have been overwhelmed by the large quantity of BPK1 in the LC-MS/MS analysis. Given this and the fact that MCP4 is a component of the cyst wall (9), we used immunoblotting to determine whether MCP4 co-IPs with BPK1. The results showed that MCP4 does indeed immunoprecipitate with the BPK1-tag strain (Fig. 4A, lane 4) and was not detected in the untagged control strain (Fig. 4A, lane 3). Thus, MCP4 also appears to form a complex that includes BPK1.

To further confirm that these proteins form a complex involving BPK1, reciprocal immunoprecipitations were performed whereby GRA8, GRA9, MAG1, and MCP4 were immunoprecipitated from bradyzoite cultures infected with a C-terminally HA-tagged version of BPK1. The results with anti-GRA8, anti-MAG1, and anti-MCP4 showed associated BPK1 at levels above those seen with control, irrelevant antibodies (Fig. 4B). The association of these proteins with the HA-tagged BPK1 negates the possibility that they associate with tagged BPK1 via the venus, 6×His, or 3×FLAG tags used in the initial IP. Immunoprecipitation of GRA7 showed no associating BPK1 above that seen with control antibodies (Fig. 4B) consistent with a lack of association between these two proteins as demonstrated above. The amount of BPK1 detected after immunoprecipitation of GRA9 was consistently above the background level, although it was substantially less than the amount precipitating with GRA8, MAG1, and MCP4 (Fig. 4B). This could be because either less of the overall GRA9 protein in the vacuole may associate with the BPK1 complex, or the polyclonal sera used for the immunoprecipitation of GRA9 may compete for the region of the protein involved in associating with the BPK1 complex. Together with the results in Fig. 2, these data demonstrate that BPK1 forms a complex that includes at least 4 known components of the PVM/cyst wall.

**Generation of a *bpk1* knockout and complemented strain.** To provide a reagent for studying the function of BPK1, a strain was created with the *BPK1* gene deleted by homologous recombination and insertion of the *HXGPRT* selectable marker (Δ*bpk1*; Fig. 5A). Correct integration of the knockout vector was indicated by growth under MPA-XAN selection and the absence of the mCherry negative selection marker (Fig. 5A) and was confirmed by PCR and sequencing using diagnostic primer pairs specific for the flanking and coding regions (see Table S1 in the supplemental material). Along with the knockout clone of the parasite, a clone from the same population was isolated that had integrated the

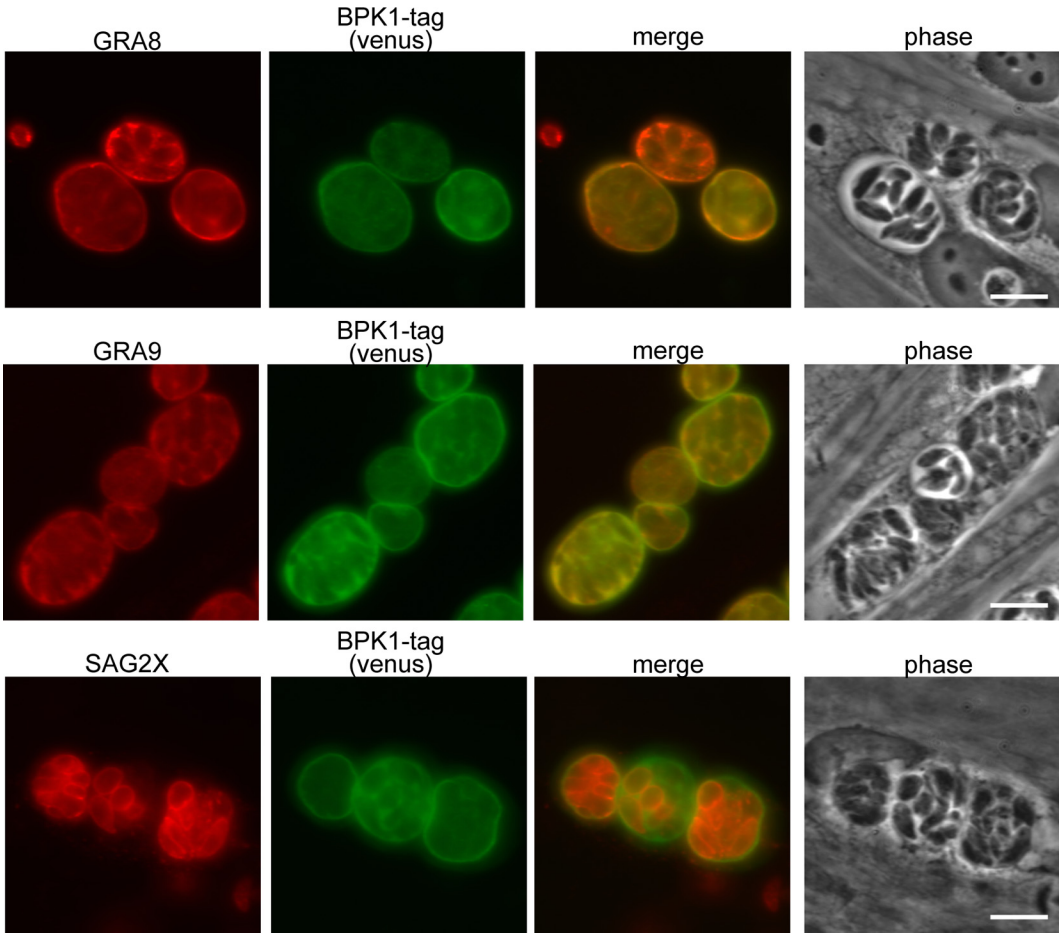


**FIG 3** Localization of GRA8, GRA9, and SAG2X in *in vitro* bradyzoite cysts at 4 dpi. BPK1-tagged parasites were grown on HFF monolayers on glass coverslips for 4 days under bradyzoite growth conditions prior to fixation. The images were obtained with antibodies to GRA8, GRA9, and SAG2X (red) or BPK1 tag (venus; green). Representative images from one of at least two experiments are shown. Bars, 10 μm.

*HXGPRT* marker without disrupting the *BPK1* locus. This strain was used as the "parental" control strain throughout these studies. To transfer (complement) the *BPK1* gene back into the Δ*bpk1* strain, the *HXGPRT* selectable marker which had been integrated into the genome by the pTKO2 vector (Fig. 5A) was first removed by transient transfection of a plasmid expressing Cre recombinase and selection for loss of HXGPRT using 6-thioxanthine (Caffaro et al., submitted); Cre recombination results in removal of the *HXGPRT* gene, as this marker is flanked by *loxP* sites in the pTKO2 vector (Fig. 5A). After passage under 6-thioxanthine selection, single clones were derived by limiting dilutions, and excision of *HXGPRT* was confirmed by PCR. The Δ*bpk1* strain was complemented with the *BPK1* locus and ~2,000 bp of the upstream promoter region by ectopic insertion as described in Materials and Methods. The levels of BPK1 expression in the knockout and complemented strain were checked by SDS-PAGE using 3 dpi bradyzoite lysates and probing with mouse polyclonal antisera raised against recombinant GST-BPK1 (Fig. 5B). The results showed similar levels of BPK1 expression in the parental and complemented strain and, as expected, no expression in the Δ*bpk1* strain (Fig. 5B). Similarly, IFA revealed that BPK1 is appropriately secreted into cysts of the complemented strain and absent from knockout cysts (Fig. 5C). Together these data confirm the generation of a Δ*bpk1* knockout strain and a complemented strain that expresses and traffics BPK1 at levels approximating the parental strain parasites.

**BPK1 plays little if any role in *in vitro* growth or cyst formation.** To determine whether BPK1 is essential for cyst formation or parasite growth *in vitro*, the knockout and parental control parasites were grown for 4 days under bradyzoite growth conditions on glass coverslips prior to fixation and probing with either DBA as a marker of the cyst wall or with antibody to the bradyzoite surface antigen SAG2X (24). No difference was detected in the ability of the Δ*bpk1* parasites to convert to the bradyzoite stage and form cysts, relative to the parental strain, as measured by the percentage of vacuoles expressing SAG2X or the number of cysts (DBA-positive vacuoles; see Fig. S1A and S1B in the supplemental material). Similarly, no difference was found in the size of the cysts formed as judged by measuring the two-dimensional area of the cyst using ImageJ software (Fig. S1C). BPK1 was also judged nonessential for growth of tachyzoites *in vitro* based on the absence of any apparent difference in growth between parental and knockout strains under tachyzoite conditions.

**BPK1 is not important for initiating an *in vivo* infection with tachyzoites.** To investigate the role of BPK1 *in vivo* during acute infection, female CBA/J mice were infected intraperitoneally (i.p.)

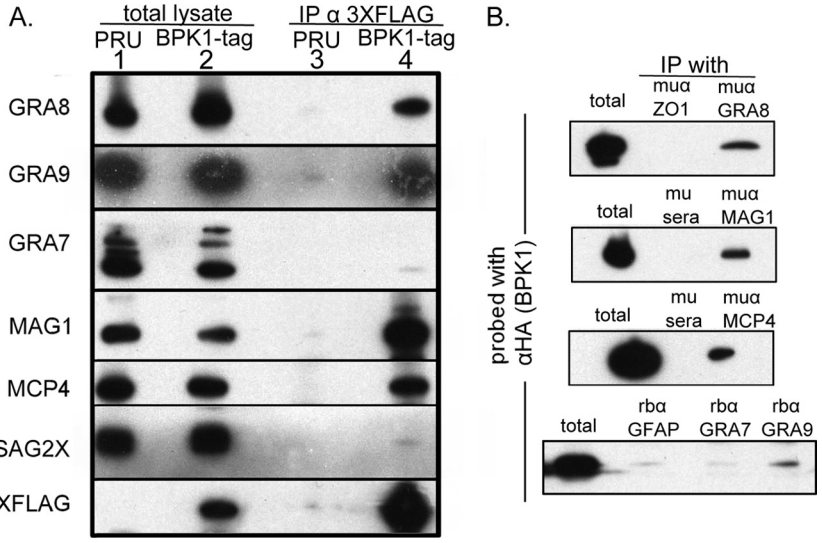


**FIG 4** BPK1 forms a complex with PVM and cyst wall proteins. (A) Immunoprecipitations were performed with mouse anti-3×FLAG monoclonal antibody (IP α 3XFLAG) against total parasite and host cell lysates after 4 days growth under bradyzoite conditions. HFF cells were infected with either the parental untagged strain (PRU) (lanes 1 and 3) or the BPK1-tag strain (lanes 2 and 4). Total lysate (lanes 1 and 2) and eluate of the co-IP (lanes 3 and 4) were analyzed by immunoblotting with antibodies specific for GRA7, -8, and -9, MAG1, MCP4, SAG2X, and 3×FLAG. (B) Immunoprecipitation with antibodies specific to GRA8, MAG1, MCP4, GRA9, or GRA7 or control antibodies (muα [mouse antibody] or rbα [rabbit antibody]) were performed on 4 dpi bradyzoite cultures infected with BPK1-HA parasites and immunoblots probed for BPK1 with monoclonal rat anti-HA-HRP antibody.

with $2.5 \times 10^4$ tachyzoites of either the parental control or knockout strains. No difference was found in weight loss or time of survival with all mice showing significant illness and comparable levels of mortality (~20%; data not shown). Thus, BPK1 appears to be unnecessary for *in vivo* growth and pathogenesis during the acute phase of infection in mice.

**BPK1 is necessary for the growth, maintenance, and/or stability of *Toxoplasma* tissue cysts *in vivo*.** To determine whether BPK1 is important for establishing and maintaining cysts during a chronic infection, mice infected with the parental, Δ*bpk1*, or complemented parasites were sacrificed at 4 or 8 wpi, and the number of cysts in the brain was determined by microscopy following staining of the cyst wall with DBA-rhodamine. No difference in cyst burden was found at 4 wpi (Fig. 6; also data not shown [5 independent experiments with parental and Δ*bpk1* strains]), indicating that BPK1 is not essential for establishing the cyst burden. To identify whether BPK1 is important for the stability or maintenance of the cyst population over time, the cyst burden was also determined at 8 wpi. The results showed fewer cysts in the mice infected with the Δ*bpk1* parasites compared to the parental or complemented strain, although variability of the data did not allow this difference to reach statistical significance (Fig. 6).

To determine the effect of deleting *BPK1* on cyst size, the diameters of cysts were measured in mouse brains infected with the control, Δ*bpk1*, and complemented strains at 4 and 8 wpi. No differences in cyst diameter between strains was found at 4 wpi (Fig. 7A). At 8 wpi, however, the Δ*bpk1* cysts were significantly smaller than the cysts of the parental and complemented strains (Fig. 7A and B). The Δ*bpk1* cysts at 8 wpi were also significantly smaller than the Δ*bpk1*, control, and complemented strain cysts at 4 wpi (Fig. 7A). These data suggest that BPK1 is necessary for the growth, maintenance, and/or stability of *Toxoplasma* tissue cysts *in vivo*.

**BPK1 knockout parasites are defective in oral infection.** While no difference in pathogenesis of the Δ*bpk1* strain was seen after i.p. injection of tachyzoites, this is not a natural route of infection by *Toxoplasma*. To determine whether BPK1 is important for oral infectivity of *Toxoplasma*, 100 or 250 *in vivo* cysts at 4 wpi were fed to naïve mice. Note that at 4 wpi, no difference in cyst size was detected between the strains, so the infective dose as measured by number of bradyzoites should be the same for all three strains. None of the orally infected mice showed signs of illness (drop in weight or death) through the acute phase of infection (i.e., the first 3 weeks; data not shown). (It was not possible to use a larger dose of cysts because the amount of infected brain material needed to achieve such a dose exceeded the capacity of the animals to ingest the material.) To determine whether these mice had become infected after oral ingestion of the cysts, sera were isolated 2 to 3 wpi and assessed for seroconversion by immunoblotting. Mice infected with the parental strain seroconverted 33% of the time when given a dose of 100 cysts (Table 2). This rate increased to 67% when the cyst dose was increased to 250 (Table 2). In contrast, only 1 of 19 mice infected with Δ*bpk1* cysts ever seroconverted, resulting in a much lower seroconversion rate for this strain in mice infected with either 100 or 250 cysts (8% and 0%, respectively; Table 2). Adding (complementing) the *BPK1* locus back into the Δ*bpk1* strain rescued this defect in oral infectivity, returning the seroconversion rates to 29% for the 100-cyst dose and 43% for the 250-cyst dose (Table 2). These data indicate that BPK1 is necessary for efficient oral infection by *Toxoplasma* bradyzoite cysts.

**BPK1 is necessary for parasite viability and ability to withstand conditions of the GI system.** Cysts formed by the Δ*bpk1* parasites are reduced in their ability to cause oral infection. As the cyst is thought to protect parasites during passage through the gastrointestinal (GI) system, this defect in oral infectivity could be due to decreased ability of the cysts and parasites to withstand such conditions. Pepsin-HCl treatment *in vitro* mimics conditions in the stomach and can be used to release bradyzoites from the cyst (4). Bradyzoites are normally resistant to this digestion process,

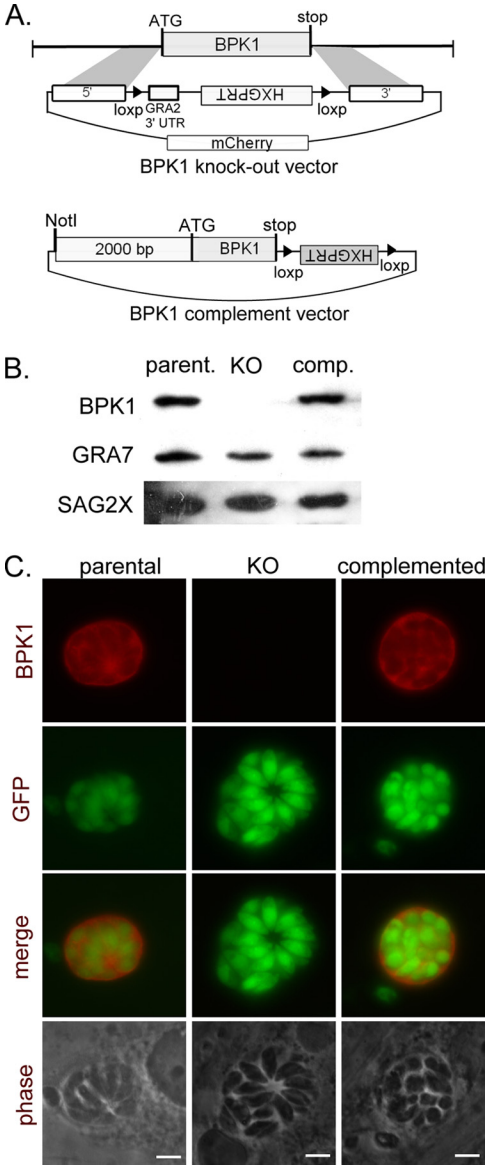


**FIG 5** Generation of a *BPK1*-knockout strain. (A) Schematic of the vector used for the double-crossover event to delete the *BPK1* coding region and replace it with a *HXGPRT* selectable marker and the complementing vector used to ectopically express BPK1. 3′ UTR, 3′ untranslated region. (B) HFF monolayers were infected with the parental (parent.), Δ*bpk1* (knockout [KO]), or complemented (comp.) strain for 3 days under bradyzoites growth conditions. For analysis by SDS-PAGE, cells were disrupted by syringe lysis and counted prior to the addition of loading buffer. A total of $5 \times 10^5$ parasite equivalents were loaded per lane and probed with antibodies specific for BPK1, GRA7, or SAG2X as described in Materials and Methods. (C) To localize BPK1 by immunofluorescence assay, cells grown under bradyzoite conditions on glass coverslips were fixed at 3 dpi and stained with mouse anti-BPK1 (red). Parasites were detected by epifluorescence for green fluorescent protein (GFP) (green). Representative images from one of at least two independent experiments are shown. Bars, 5 μm.

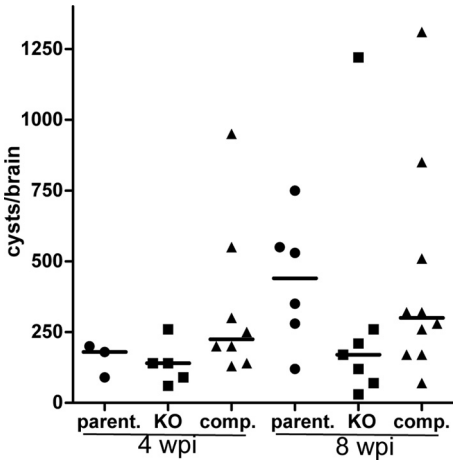


**FIG 6** Quantification of cyst burden *in vivo*. Female CBA/J mice were infected i.p. with $2.5 \times 10^4$ parental (parent.), Δ*bpk1* (KO), or complemented (comp.) tachyzoites. At 4 and 8 weeks postinfection (wpi), the brains were processed and the bradyzoite cysts were stained with DBA as described in Materials and Methods. One-fifth of the total brain was counted. Data shown are total cyst count per brain pooled from two independent experiments. Each symbol represents the value for an individual mouse. The median for the group is indicated by the black bar.

compared to tachyzoites, so this assay was used to assess the possible role of BPK1 in oral infectivity. To do this, cysts from the brains of mice infected with the parental, Δ*bpk1*, and complemented strains were isolated 4 wpi by Percoll gradient and enumerated by DBA staining and counting on an inverted microscope. Ten to 30 cysts were treated with pepsin-HCl, aliquots were removed, neutralized at 30 s and 10 min, and added to confluent HFF monolayers in triplicate. DNA was extracted from an additional aliquot of the pepsin-treated cysts, and qPCR of the B1 gene (28) was used to quantify the number of parasites. Following 9 days of growth, the number of plaques (each indicating a viable parasite) was determined and compared to the total number of "input" parasites, as determined by qPCR, to determine the percent viability. After 10 min of pepsin-HCl treatment, Δ*bpk1* parasites were significantly less viable than the parental and complemented parasite strains (Fig. 8A). A trend toward reduced viability in the knockout (KO) strain was also seen with 30 s of pepsin treatment compared to the parental and complemented strains ($P = 0.076$ and $P = 0.051$, respectively). These data show that fewer Δ*bpk1* parasites survive after pepsin-HCl digestion of the cyst.

Although the Δ*bpk1* parasites had reduced viability after pepsin-HCl treatment, this assay cannot differentiate between parasites that were disabled prior to the treatment versus the effect of the treatment itself. We found other methods of releasing parasites from the cyst (e.g., syringe lysis) to be highly variable and generally much less effective than pepsin digestion (data not shown), and thus, quantifying the number of viable parasites prior to pepsin digestion was not feasible. To determine whether the Δ*bpk1* parasites were more susceptible to the pepsin-acid conditions, therefore, the percent change in viability was determined by direct comparison of the plaque counts at 30 s and 10 min. As expected, all strains had significantly reduced parasite viability with longer incubation in the pepsin-HCl digestion solution (10 min versus 30 s; Fig. 8A). The viability of the Δ*bpk1* parasites, however, showed a significantly greater decrease with longer pepsin-HCl treatment relative to the parental and complemented controls (Fig. 8B), indicating a greater susceptibility to the digestion conditions and, thus, a role for BPK1 in resistance to this treatment.

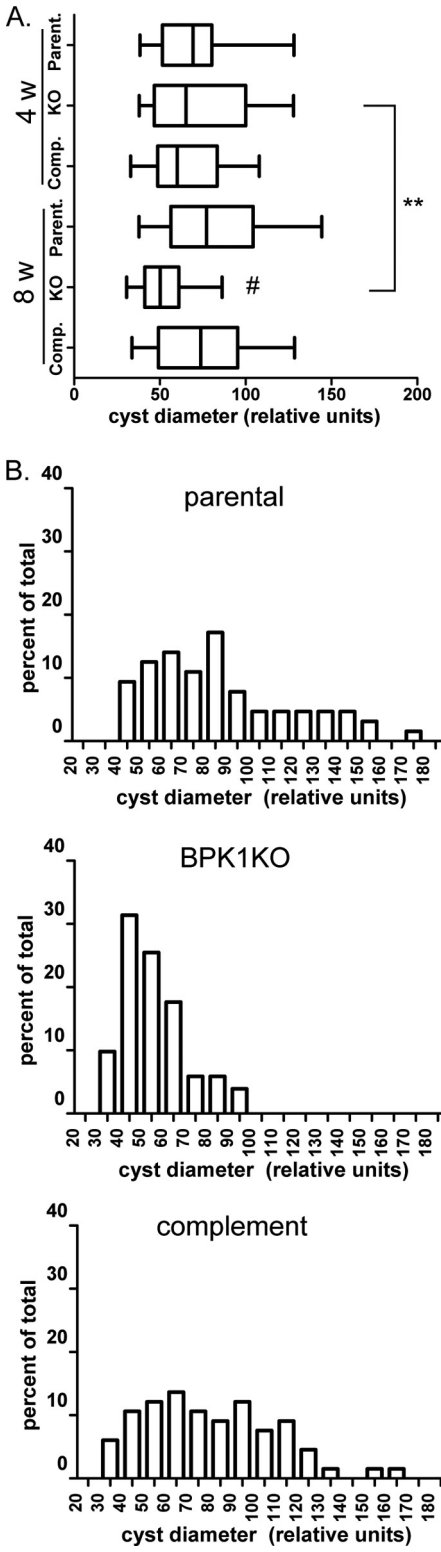


**FIG 7** Δ*bpk1* cysts are significantly smaller 8 weeks (8 w) postinfection. The images of DBA-stained cysts were taken with an inverted microscope as described in Materials and Methods. Ten to 20 cysts each from at least 3 independently processed brains were imaged for mice infected with the parental (parent.), Δ*bpk1* (KO), and complemented (comp.) strains, and the diameter of the cyst was ascertained using Adobe Photoshop. (A) Box plots show the median percentage and 25th and 75th percentiles with whiskers indicating the 5th and 95th percentiles. The # symbol indicates a significant difference ($P < 0.01$) in the 8 wpi Δ*bpk1* cysts relative to all other groups. The pair of asterisks indicates a significant difference ($P < 0.01$) between 4 and 8 wpi Δ*bpk1* cysts (Mann-Whitney test). (B) Histogram (bin of 10) of relative cyst sizes at 8 wpi. The data are representative of at least two independent experiments.

**TABLE 2** Seroconversion rates after oral infection with *in vivo* bradyzoite tissue cysts

| Strain | Cyst dose[a] | No. seropositive/total[b] | % Seropositive[c] |
|---|---|---|---|
| Parental | 100 | 5/15 | 33 |
| | 250 | 4/6 | 67 |
| Δ*bpk1* | 100 | 1/13 | 8 |
| | 250 | 0/6 | 0 |
| Complemented | 100 | 2/7 | 29 |
| | 250 | 3/7 | 43 |

[a] Cyst dose indicates the number of cysts fed to each mouse. Cysts were enumerated in brain mash by staining with the DBA lectin and counting as described in Materials and Methods.
[b] Number of seropositive mice as determined by Western blotting as described in Materials and Methods shown as a ratio over the total number of mice fed. Pooled data from 6 experiments are shown for the parental and complemented strains. Pooled data from 3 experiments are shown for the complemented strain.
[c] Percentage of mice that seroconverted compared to the total number of mice fed.

## DISCUSSION

Here we investigate the function of the bradyzoite-expressed pseudokinase BPK1 *in vitro* and *in vivo*. BPK1 is a component of the cyst wall and is upregulated in bradyzoites relative to tachyzoites and sporozoites (9, 35). This expression specifically in bradyzoites suggests it may have an important function in bradyzoite biology or the structure or function of the tissue cyst. Pseudokinases have been shown to have important regulatory and scaffolding functions in other systems (11). Indeed, in *Toxoplasma*, the injected pseudokinase ROP5 has been recently shown to associate with host Irga6 in such a way that it can be phosphorylated and inactivated by the active kinase ROP18 (36). It is interesting to hypothesize that BPK1 may also be regulating the function of an active kinase within the bradyzoite tissue cyst, but we detected no such protein in the co-IP (Fig. 2 and 4), nor has an active kinase yet been described within the cyst wall or lumen.

Few components of the cyst wall have been identified, and nothing is known about their function. Coimmunoprecipitation assays of BPK1 described here reveal an interaction between BPK1 and four protein components of the cyst wall and parasitophorous vacuolar membrane, GRA8, GRA9, MAG1, and MCP4, although it is not known at this time which of these are direct versus indirect interactions (i.e., BPK1 could be part of a larger protein complex involving these components but not interacting with any of them directly). Pseudokinases have been shown to mediate multiprotein complexes by facilitating conformational changes in the bound partner(s) (11). Thus, BPK1 may be key to the formation of a protein complex, even without directly interacting with each component perhaps through acting as a bridge between the cyst matrix, cyst wall and PVM. Further experimentation, however, will be needed to determine whether this is indeed its role and to explore the possibility that the cyst wall is a single, interconnected entity and that all proteins in it will coprecipitate with all others. Likewise, further work will be needed to determine

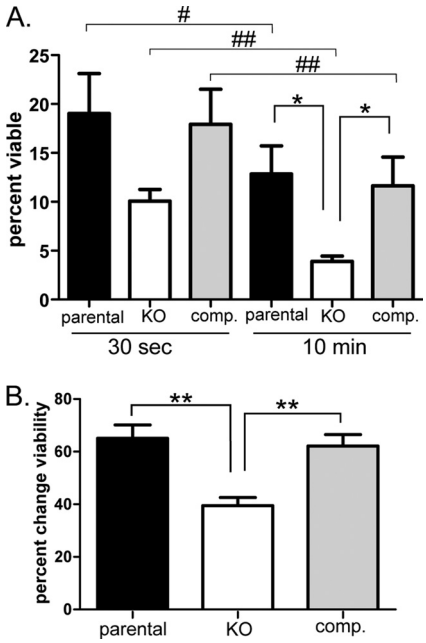


**FIG 8** Parasites from Δ*bpk1* cysts are less viable after pepsin-HCl treatment. Cysts were isolated 4 wpi from the brains of mice infected with the parental, Δ*bpk1* (KO), or complemented (comp.) strain and incubated in 0.05 mg/ml pepsin-HCl for 30 s or 10 min prior to plaquing on confluent HFF monolayers. (A) Plaque counts indicating viable parasites were compared to the total number of input parasites as determined by qPCR of the B1 gene (see Materials and Methods) and plotted as average plus standard error of the mean (SEM) (error bar). (B) Comparison of 10 min and 30 s plaque counts to determine the change in viability with longer time of pepsin treatment, plotted as average plus SEM. Data shown for each *Toxoplasma* strain are the result of 2 independent infections and 5 to 7 independently processed and treated brains. Values that are significantly different are indicated by brackets and symbols as follows: *, $P < 0.02$; **, $P < 0.01$; #, $P < 0.05$; ##, $P < 0.01$. The asterisks indicate that the statistical significance was indicated by an unpaired *t* test; the pound symbols indicate that the statistical significance was indicated by a paired *t* test.

whether the other three proteins identified in the initial immunoprecipitation, TgHSP70/BiP, SRS44, and TgSPATR, have a specific interaction with the BPK1 complex (although it should be noted that HSP70 proteins are frequently present in immunoprecipitations because of their chaperonin role and general protein-binding capacity and so are typically not considered to be "specific" interactors).

BPK1 associates with dense granule components of the PVM, specifically GRA8 and GRA9, without significantly associating with another abundantly secreted dense granule protein, GRA7. The roles of GRA8 and GRA9 in tachyzoite or bradyzoite vacuoles are currently unknown. Data presented here, however, could suggest that these proteins are important in the formation or function of the cyst; i.e., it could be that the deleterious effect of the absence of BPK1 on 8 wpi *in vivo* cysts is actually mediated through downstream effects on its interacting partners. Indeed, other dense-granule-secreted proteins such as GRA4 and GRA6 have been shown to be important for establishing and/or maintaining cysts *in vivo* (37). Investigation of this possibility will require generation and testing of knockouts of GRA8 and GRA9.

At 8 wpi, mice infected with the Δ*bpk1* strain showed a reduction in overall cyst burden. While this reduction did not reach the level of statistical significance due to variability in the cyst burden, these data are reminiscent of the phenotype seen with other mutants harboring deletions of bradyzoite-specific genes, including bradyzoite surface antigens, SRS9 (15) and SAG2CDXY (24), and the heat shock protein BAG1 (38), as well as the PVM-associated proteins GRA4 and GRA6 which are expressed in both the tachyzoite and bradyzoite stages (37). This suggests that multiple factors involved in bradyzoite development and/or the structure and function of the vacuole are necessary for establishing and maintaining tissue cysts.

Our results found that at 8 wpi *in vivo*, cysts of the Δ*bpk1* mutant were significantly smaller than cysts of the parental or complemented strains. Components of the immune system such as major histocompatibility complex (MHC) class I are known to affect the ability of the host to regulate cyst burden (39). It is unclear at this time whether deletion of *BPK1* leads to more efficient clearance of the mature (larger) cysts by the host, or if clearance occurs after rupture of cysts unable to be maintained by the Δ*bpk1* parasites due to size or age. It is also formally possible that, in the absence of BPK1, cysts may shrink in size. Extensive *in vivo* analysis will be needed to further resolve the specific mechanisms underlying the observed differences in cyst size and number.

BPK1 is necessary for the efficient initiation of a new oral infection by tissue cysts. Disruption of the genes encoding BRP1 (40), SAG2CDXY (24), and SRS9 (15) all impact cyst burden but did not result in any detectable difference in oral infectivity. It is important to note, however, that for examination of the *SAG2CDXY* and *BRP1* knockout parasites, oral gavage was used as the method of infection compared to "natural feeding" (cyst-containing tissue placed on food that is naturally ingested) (24, 40). Since oral gavage has been found to be an inconsistent means of infection, often resulting in initial parasite growth in regions outside the gut of the mouse (41), we cannot exclude the possibility that a defect in oral infectivity would be found in these strains using alternative feeding methods. Disruption of the gene encoding *T. gondii* calcium-dependent protein kinase 3 (TgCDPK3), however, produces a phenotype similar to the phenotype of the BPK1 mutants described here with a decreased ability to establish a persistent infection in the brain after oral infection with bradyzoite cysts (42, 43), albeit this TgCDPK3 work was with gavage feeding and used cysts produced *in vitro*. These authors did not explore the mechanism behind this lack of oral infectivity, but TgCDPK3 is a key signaling enzyme involved in sensitivity to calcium ionophores and, in particular, to ionophore-induced egress (43). There is no reason to suspect an interaction between TgCDPK3 and BPK1, and their respective phenotypes in terms of oral infectivity could reflect a block at any of several steps in the progression from an acute infection to a persistent infection.

There are at least two means through which BPK1 could be protecting the parasites from the pepsin-acid conditions of the GI system: integrity of the cyst wall and/or of the bradyzoites themselves (i.e., Δ*bpk1* parasites might be intrinsically more sensitive to the pepsin-HCl, once released). The localization of BPK1 within the cyst wall favors the former, but we cannot exclude the latter, and further, detailed analysis of the cyst stage will be needed to discriminate between these two possibilities. Regardless, the data presented here identify the pseudokinase BPK1 as vital to the persistence and subsequent oral infectivity of the bradyzoite-contain-

ing tissue cyst, a crucial stage in the life cycle of *Toxoplasma gondii* and many related parasites.

## ACKNOWLEDGMENTS

This work was supported in part by the NIH (AI 41014). K.R.B. was funded by NIH training grant T32 AI7328 and a grant from the American Cancer Society. P.W.B. was supported by NIH grant R01 AI078947 (to Matthew Bogyo, Department of Pathology, Stanford University School of Medicine) and a Burroughs Wellcome new investigator in pathogenesis award (to Matthew Bogyo).

## REFERENCES

1. **Montoya J, Kovacs J, Remington J.** 2005. *Toxoplasma gondii*, p 3170–3197. *In* Mandell G, Bennett J, Dolin R (ed), Principles and practice of infectious diseases, 6th ed. Elsevier, Philadelphia, PA.
2. **Martino R, Maertens J, Bretagne S, Rovira M, Deconinck E, Ullmann AJ, Held T, Cordonnier C.** 2000. Toxoplasmosis after hematopoietic stem cell transplantation. Clin. Infect. Dis. **31**:1188–1195.
3. **Pruitt AA.** 2004. Central nervous system infections in cancer patients. Semin. Neurol. **24**:435–452.
4. **Dubey JP, Lindsay DS, Speer CA.** 1998. Structures of *Toxoplasma gondii* tachyzoites, bradyzoites, and sporozoites and biology and development of tissue cysts. Clin. Microbiol. Rev. **11**:267–299.
5. **Weiss LM, Kim K.** 2007. Bradyzoite development, p 341–366. *In* Weiss LM, Kim K (ed), *Toxoplasma gondii*. The model apicomplexan: perspectives and methods. Academic Press, London, United Kingdom.
6. **Zhang YW, Halonen SK, Ma YF, Wittner M, Weiss LM.** 2001. Initial characterization of CST1, a *Toxoplasma gondii* cyst wall glycoprotein. Infect. Immun. **69**:501–507.
7. **Craver MP, Rooney PJ, Knoll LJ.** 2010. Isolation of *Toxoplasma gondii* development mutants identifies a potential proteophosphoglycan that enhances cyst wall formation. Mol. Biochem. Parasitol. **169**:120–123.
8. **Parmley SF, Yang S, Harth G, Sibley LD, Sucharczuk A, Remington JS.** 1994. Molecular characterization of a 65-kilodalton *Toxoplasma gondii* antigen expressed abundantly in the matrix of tissue cysts. Mol. Biochem. Parasitol. **66**:283–296.
9. **Buchholz KR, Fritz HM, Chen X, Durbin-Johnson B, Rocke DM, Ferguson DJ, Conrad PA, Boothroyd JC.** 2011. Identification of tissue cyst wall components by transcriptome analysis of in vivo and in vitro Toxoplasma gondii bradyzoites. Eukaryot. Cell **10**:1637–1647.
10. **Hanks SK, Hunter T.** 1995. Protein kinases 6. The eukaryotic protein kinase superfamily: kinase (catalytic) domain structure and classification. FASEB J. **9**:576–596.
11. **Boudeau J, Miranda-Saavedra D, Barton GJ, Alessi DR.** 2006. Emerging roles of pseudokinases. Trends Cell Biol. **16**:443–452.
12. **Fux B, Nawas J, Khan A, Gill DB, Su C, Sibley LD.** 2007. *Toxoplasma gondii* strains defective in oral transmission are also defective in developmental stage differentiation. Infect. Immun. **75**:2580–2590.
13. **Ong YC, Reese ML, Boothroyd JC.** 2010. *Toxoplasma* rhoptry protein 16 (ROP16) subverts host function by direct tyrosine phosphorylation of STAT6. J. Biol. Chem. **285**:28731–28740.
14. **Soldati D, Boothroyd JC.** 1993. Transient transfection and expression in the obligate intracellular parasite *Toxoplasma gondii*. Science **260**:349–352.
15. **Kim SK, Karasov A, Boothroyd JC.** 2007. Bradyzoite-specific surface antigen SRS9 plays a role in maintaining *Toxoplasma gondii* persistence in the brain and in host control of parasite replication in the intestine. Infect. Immun. **75**:1626–1634.
16. **Donald RG, Carter D, Ullman B, Roos DS.** 1996. Insertional tagging, cloning, and expression of the *Toxoplasma gondii* hypoxanthine-xanthine-guanine phosphoribosyltransferase gene. Use as a selectable marker for stable transformation. J. Biol. Chem. **271**:14010–14019.
17. **Reese ML, Boothroyd JC.** 2009. A helical membrane-binding domain targets the Toxoplasma ROP2 family to the parasitophorous vacuole. Traffic **10**:1458–1470.
18. **Dix MM, Simon GM, Cravatt BF.** 2008. Global mapping of the topography and magnitude of proteolytic events in apoptosis. Cell **134**:679–691.
19. **Bowyer PW, Simon GM, Cravatt BF, Bogyo M.** 2011. Global profiling of proteolysis during rupture of *Plasmodium falciparum* from the host erythrocyte. Mol. Cell. Proteomics **10**:M110.001636. doi:10.1074/mcp.M110.001636.
20. **Fritz HM, Bowyer PW, Bogyo M, Conrad PA, Boothroyd JC.** 2012. Proteomic analysis of fractionated *Toxoplasma* oocysts reveals clues to their environmental resistance. PLoS One **7**:e29955. doi:10.1371/journal.pone.0029955.
21. **Tabb DL, McDonald WH, Yates JR, III.** 2002. DTASelect and Contrast: tools for assembling and comparing protein identifications from shotgun proteomics. J. Proteome Res. **1**:21–26.
22. **Adjogble KD, Mercier C, Dubremetz JF, Hucke C, Mackenzie CR, Cesbron-Delauw MF, Daubener W.** 2004. GRA9, a new *Toxoplasma gondii* dense granule protein associated with the intravacuolar network of tubular membranes. Int. J. Parasitol. **34**:1255–1264.
23. **Carey KL, Donahue CG, Ward GE.** 2000. Identification and molecular characterization of GRA8, a novel, proline-rich, dense granule protein of Toxoplasma gondii. Mol. Biochem. Parasitol. **105**:25–37.
24. **Saeij JP, Arrizabalaga G, Boothroyd JC.** 2008. A cluster of four surface antigen genes specifically expressed in bradyzoites, SAG2CDXY, plays an important role in *Toxoplasma gondii* persistence. Infect. Immun. **76**:2402–2410.
25. **Dunn JD, Ravindran S, Kim SK, Boothroyd JC.** 2008. The *Toxoplasma gondii* dense granule protein GRA7 is phosphorylated upon invasion and forms an unexpected association with the rhoptry proteins ROP2 and ROP4. Infect. Immun. **76**:5853–5861.
26. **Brymora A, Valova VA, Robinson PJ.** 2004. Protein-protein interactions identified by pull-down experiments and mass spectrometry. Curr. Protoc. Cell Biol. Chapter 17, Unit 17.5. doi:10.1002/0471143030.cb1705s22.
27. **Huskinson-Mark J, Araujo FG, Remington JS.** 1991. Evaluation of the effect of drugs on the cyst form of *Toxoplasma gondii*. J. Infect. Dis. **164**:170–171.
28. **Noor S, Habashy AS, Nance JP, Clark RT, Nemati K, Carson MJ, Wilson EH.** 2010. CCR7-dependent immunity during acute *Toxoplasma gondii* infection. Infect. Immun. **78**:2257–2263.
29. **Dzierszinski F, Nishi M, Ouko L, Roos DS.** 2004. Dynamics of *Toxoplasma gondii* differentiation. Eukaryot. Cell **3**:992–1003.
30. **Hager KM, Striepen B, Tilney LG, Roos DS.** 1999. The nuclear envelope serves as an intermediary between the ER and Golgi complex in the intracellular parasite *Toxoplasma gondii*. J. Cell Sci. **112**(Part 16):2631–2638.
31. **Kawase O, Nishikawa Y, Bannai H, Igarashi M, Matsuo T, Xuan X.** 2010. Characterization of a novel thrombospondin-related protein in *Toxoplasma gondii*. Parasitol. Int. **59**:211–216.
32. **Huynh MH, Carruthers VB.** 2009. Tagging of endogenous genes in a *Toxoplasma gondii* strain lacking Ku80. Eukaryot. Cell **8**:530–539.
33. **Jacobs D, Dubremetz JF, Loyens A, Bosman F, Saman E.** 1998. Identification and heterologous expression of a new dense granule protein (GRA7) from *Toxoplasma gondii*. Mol. Biochem. Parasitol. **91**:237–249.
34. **Friedrich N, Santos JM, Liu Y, Palma AS, Leon E, Saouros S, Kiso M, Blackman MJ, Matthews S, Feizi T, Soldati-Favre D.** 2010. Members of a novel protein family containing microneme adhesive repeat domains act as sialic acid-binding lectins during host cell invasion by apicomplexan parasites. J. Biol. Chem. **285**:2064–2076.
35. **Fritz HM, Buchholz KR, Chen X, Durbin-Johnson B, Rocke DM, Conrad PA, Boothroyd JC.** 2012. Transcriptomic analysis of toxoplasma development reveals many novel functions and structures specific to sporozoites and oocysts. PLoS One **7**:e29998. doi:10.1371/journal.pone.0029998.
36. **Fleckenstein MC, Reese ML, Konen-Waisman S, Boothroyd JC, Howard JC, Steinfeldt T.** 2012. A *Toxoplasma gondii* pseudokinase inhibits host IRG resistance proteins. PLoS Biol. **10**:e1001358. doi:10.1371/journal.pbio.1001358.
37. **Fox BA, Falla A, Rommereim LM, Tomita T, Gigley JP, Mercier C, Cesbron-Delauw MF, Weiss LM, Bzik DJ.** 2011. Type II *Toxoplasma gondii* KU80 knockout strains enable functional analysis of genes required for cyst development and latent infection. Eukaryot. Cell **10**:1193–1206.
38. **Zhang YW, Kim K, Ma YF, Wittner M, Tanowitz HB, Weiss LM.** 1999. Disruption of the Toxoplasma gondii bradyzoite-specific gene BAG1 decreases in vivo cyst formation. Mol. Microbiol. **31**:691–701.
39. **Brown CR, Hunter CA, Estes RG, Beckmann E, Forman J, David C, Remington JS, McLeod R.** 1995. Definitive identification of a gene that confers resistance against *Toxoplasma* cyst burden and encephalitis. Immunology **85**:419–428.
40. **Schwarz JA, Fouts AE, Cummings CA, Ferguson DJ, Boothroyd JC.**

2005. A novel rhoptry protein in *Toxoplasma gondii* bradyzoites and merozoites. Mol. Biochem. Parasitol. **144**:159–166.
41. **Boyle JP, Saeij JP, Boothroyd JC.** 2007. *Toxoplasma gondii*: inconsistent dissemination patterns following oral infection in mice. Exp. Parasitol. **116**:302–305.
42. **Lavine MD, Knoll LJ, Rooney PJ, Arrizabalaga G.** 2007. A *Toxoplasma gondii* mutant defective in responding to calcium fluxes shows reduced in vivo pathogenicity. Mol. Biochem. Parasitol. **155**:113–122.
43. **Garrison E, Treeck M, Ehret E, Butz H, Garbuz T, Oswald BP, Settles M, Boothroyd J, Arrizabalaga G.** 2012. A forward genetic screen reveals that calcium-dependent protein kinase 3 regulates egress in *Toxoplasma*. PLoS Pathog. **8**:e1003049. doi:10.1371/journal.ppat.1003049.